CHIMIA 2001, 55, No. 10

Chimia 55 (2001) 844–851

ISSN 0009–4293

Towards Biomolecular Structure Determination by High-Resolution Solid-State NMR: Assignment of Solid Peptides

Andreas Detken, Matthias Ernst, and Beat H. Meier*

Abstract: High-resolution solid-state NMR is rapidly evolving into a tool for determining the structure of biomolecules in solid phase, thereby opening up avenues for studying systems which are difficult to access by other methods. In this contribution, we focus on assigning the resonances of a uniformly isotope-enriched peptide or protein to its primary structure. This represents a first step towards the goal of determining the complete three-dimensional structure of proteins by solid-state NMR. The assignment strategy relies on polarization-transfer experiments involving ^{13}C and ^{15}N spins. The prospects for structural studies based on such assignments are discussed.

Keywords: Assignment · Polarization transfer · Solid-state NMR

1. Biomolecular Structures by Solid-state NMR – Why and How?

The solid-state NMR group in Physical Chemistry at ETH Zürich focuses on methodical developments in solid-state NMR and on applications of these methods in chemistry, biochemistry, and materials science. In this article, we discuss recent progress towards structure determination of solid, but not necessarily crystalline, peptides and proteins. An overview of other projects and the available instrumentation is given on the web site *http://www.nmr.ethz.ch*.

The presently most successful approaches to biomolecular structure determination with atomic resolution encompass mainly X-ray diffraction, developed continuously since the 1920s, and liquid-state NMR, which became a routine tool after the introduction of two-dimensional methods around 1980. With X-ray diffraction [1], structures of molecules of up to a few hundred kDa molecular weight have been solved. High-quality single crystals with dimensions of at least several micrometers are needed for this, a requirement which is not always easy to fulfill. Liquid-state NMR, on the other hand, can deliver atomic-resolution structures of proteins in solution [2][3]. Structures from proteins with sizes up to about 50 kDa have been obtained; for multimers, larger structures have been determined using the recently developed TROSY technique [4][5]. NMR is a relatively insensitive method that requires a relatively concentrated protein solution (typically in the millimolar range) in order to obtain sufficient signal intensities. High concentrations may, however, lead to aggregation of the solute.

Most of the high-resolution structures determined so far by either X-ray diffraction or liquid-state NMR are of proteins with a roughly globular shape, and, for example, only a few structures of the large class of membrane-spanning proteins (often with an elongated shape) are known.

There is strong interest in studying structural and contractible proteins, (*e.g.* silk, keratin, actin or resilin) and membrane proteins in their native environment, *i.e.* integrated into a lipid membrane. 'Solid-state' NMR has the potential of accessing the structure of proteins and other biomolecules which are insoluble and which do not form large high-quality crystals, and it allows in principle the study of membrane proteins in their native environment. These membrane systems are, of course, by no means 'solid'. The high degree of orientational order leads, however, to spectroscopic properties similar to those of solid samples. Unlike X-ray diffraction, solid-state NMR does not require long-range order in the sample, and spectra from non-crystalline or liquid-crystalline samples can be obtained and interpreted.

The interactions that lead to line splittings and shifts in the NMR spectrum can be classified into isotropic and anisotropic interactions depending whether they depend on the orientation of the system (*e.g.* molecule) to be investigated with respect to the direction of the applied magnetic field. There are two isotropic interactions, the isotropic chemical shift and the scalar coupling, which are usually important in organic or biological solids. They carry information about covalently or hydrogen-bonded neighbors, the chemical environment and structural details (*e.g.* bond and torsion angles). Anisotropic interactions include the magnetic dipole–dipole interaction (giving internuclear distances) and the chemical-shift anisotropy (CSA).

*Correspondence: Prof. Dr. B.H. Meier
Department of Chemistry
Swiss Federal Institute of Technology
ETH Hönggerberg
CH-8093 Zürich
Tel.: +41 1 632 4401
Fax: +41 1 632 1621
E-Mail: beat.meier@nmr.phys.chem.ethz.ch

CHIMIA 2001, 55, No. 10

The line positions in the NMR spectra of molecules in isotropic liquid phase are determined only by the isotropic interactions. The anisotropic interactions are averaged out by the rapid tumbling of the molecules and are reflected only in the relaxation rates. In a rigid solid, in contrast, all anisotropic interactions are present at full strength. This usually leads to extended, strongly coupled spin systems which exhibit broad resonances which are difficult to record and interpret. Furthermore, the spatial anisotropy leads to further line broadenings for powdered samples. There are, however, a number of selective averaging techniques that eliminate the influence of some interactions in the spin system by rf irradiation and/or sample spinning. The effect of these manipulations is the same as if one would simplify the Hamiltonian operator that contains the spin interactions. Using different pulse sequence elements, a 'designer Hamiltonian' can be produced and 'high-resolution' spectra can be recorded.

There are, however, a number of different approaches to studying structural features of biomolecules by solid-state NMR. Some of these approaches do not require high spectral resolution. As an example, we have recently determined the local structure of spider dragline silk by directly cross-correlating the broad distributions of static single-quantum and double-quantum frequencies [6].

An important class of systems which exhibit both liquid-state and solid-state features are oriented phospholipid bilayers or bicelles. These systems provide an ideal environment for the study of membrane-bound proteins. The technology to study such systems by NMR is, in many respects, the same as for the study of solids. All intermolecular anisotropic interactions are present even if they are somewhat scaled. Intermolecular interactions are, on the other hand, averaged out.

In this article, we concentrate on high-resolution techniques for powdered rigid solids; they rely on averaging out the anisotropic interactions (and thus achieving high resolution) by magic-angle sample rotation (MAS) [7]. This technique involves rapidly spinning the sample around an axis inclined by the 'magic angle' θ_m=54.7° relative to the external magnetic field. An MAS rotor, which serves as the sample container, is schematically depicted in Fig. 1. For each chemically inequivalent nucleus in the sample, NMR of a sample under MAS leads to a spectrum with a centerband at approximately the isotropic chemical-shift position plus a family of sidebands spaced by the MAS frequency (neglecting homogeneous broadening effects). Usually one is interested only in the centerband, which gets most intense if the MAS frequency is higher than the anisotropy of the chemical shielding interaction. This anisotropy scales linearly with the static magnetic field and is in the order of 25 kHz for aromatic and carbonyl ^{13}C nuclei in a modern high-field magnet with a field strength of 14 Tesla (corresponding to a proton Larmor frequency of 600 MHz). Furthermore, it is desirable that the sidebands do not overlap with the centerbands of other nuclei. Most conveniently, the MAS frequency is thus chosen larger than the isotropic chemical-shift range of the sample, which for the ^{13}C nuclei of a biomolecular sample in a 14 Tesla field is around 30 kHz. Therefore, 'rapid' MAS with spinning frequencies of at least 30 kHz is often advantageous. Such spinning frequencies can routinely be attained with commercial MAS rotors, typically with 2.5 mm outer diameter.

Despite high spinning frequencies, the achievable resolution in the ^1H spectrum is presently very limited due to the strong homonuclear dipolar interactions among the protons, which are not sufficiently averaged by MAS. In contrast to liquid-state work, high-resolution solid-state NMR work on biomolecules must, therefore, be based mainly on ^{13}C and ^{15}N resonances. This necessitates isotopic labeling because of the low natural abundance and of the low sensitivity of the two nuclei. For *selectively* (sparsely) labeled biomolecules, established MAS techniques allow us to measure distances and torsion angles between molecular segments containing selectively labeled spins, thereby yielding structural information (see *e.g.* [8–13]). However, selective labeling is laborious and expensive. High-resolution solid-state NMR methods for structure determination of *uniformly* labeled biomolecules are, therefore, highly desirable.

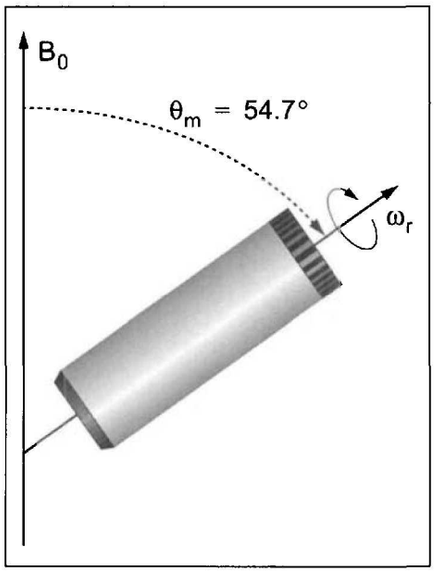

Fig. 1. Schematic drawing of an MAS rotor which is spun about an axis inclined by an angle θ_m=54.7° with respect to the direction of the static magnetic field B_0. The rotor is driven by pressured air and uses air bearings to minimize friction. Typical maximum spinning frequencies with modern rotors are 32 kHz for standard 2.5 mm o.d. spinning systems and 50 kHz with experimental 2 mm o.d. spinning systems.

This sets the framework for the present paper: we will discuss some first steps towards structure determination in solid, uniformly labeled peptides under the conditions of rapid MAS. Specifically, we will focus on methods for the sequential assignment of ^{13}C and ^{15}N resonances, which stands at the start of almost any structural investigation.

These methods will be illustrated on two examples. The first is antamanide (Fig. 2), a cyclic decapeptide which in nature can be found in small quantities in the poisonous mushroom *amanita phalloides* ('green deathcap') [14]. It acts as an antidote to the phallotoxins contained in the same mushroom [15]. The structure of antamanide is known from both X-ray diffraction [16] and liquid-state NMR [17][18], which makes it an ideal test system for comparing the advantages and disadvantages of different methods. We have obtained what may be called a 'high-resolution' solid-state NMR spectrum and the corresponding resonance assignment of antamanide [19]. The second sample which we will discuss is the 62-residue SH3 domain of chicken α-spectrin. SH3 domains are present in many proteins that are involved in signal transduction or in membrane–cytoskeleton interactions [20]. The structure of the chicken α-spectrin SH3 domain is known from X-ray diffraction [21] and liquid-state NMR [22], and we use a sample of that domain as a model compound representing a peptide somewhat larger than antamanide. An almost complete assignment of the ^{13}C and ^{15}N resonances of this domain by solid-state NMR was recently achieved by Pauli *et al.* [23].

In section 2, we will discuss the requirements imposed on the quality of a protein or peptide sample, as the quality of peptide microcrystals often determines

CHIMIA 2001, 55, No. 10

the resolution of solid-state NMR spectra. In the subsequent sections, selected experiments will be discussed which can be used for resonance assignment. In section 3, the use of homonuclear correlation techniques for the assignment of resonances to amino-acid spin systems will be illustrated. In section 4, it will be shown how the amino-acid spin systems can then be connected in a sequence-specific manner by heteronuclear correlation spectroscopy. We will conclude by briefly discussing the prospects for structure determination in uniformly labeled samples once the assignments have been obtained.

2. Obtaining Sufficient Resolution: Sample Preparation

Sufficient resolution in the one-dimensional or multi-dimensional NMR spectrum is a prerequisite for resonance assignments. Ideally, each chemically distinct (carbon or nitrogen) nucleus in the peptide gives a distinct resonance, and no overlap between resonances from different nuclei exists. To be able to distinguish the resonances from the many hundred nuclei in a peptide molecule, narrow resonance lines are required ('high resolution'). For many samples of biological interest, the resolution-limiting factor is the sample preparation rather than residual line broadening due to 'imperfect' NMR experiments (*e.g.* finite MAS frequency or insufficient proton decoupling field strength). The influence of sample preparation on the quality of the spectra is illustrated in Fig. 3, where ^{13}C and ^{15}N spectra of uniformly labeled antamanide are shown for two different sample preparation techniques. The red spectra were obtained from a sample which was freeze-dried (lyophilized) from an aqueous solution, a technique which is often used to prepare solid biomaterial. Lyophilization results in a heterogeneous local environment yielding a relatively broad distribution of resonances. Clearly, resonance assignment will be difficult for such a sample.

Much narrower lines are obtained for a microcrystalline sample obtained by controlled recrystallization (green traces). Apart from higher resolution, such a structurally homogeneous sample yields a much improved signal-to-noise ratio because the same total intensity is now concentrated in relatively few, often well-resolved resonances. The typical linewidths in these spectra are 60–100 Hz (0.4–0.7 ppm) for the ^{13}C resonances and

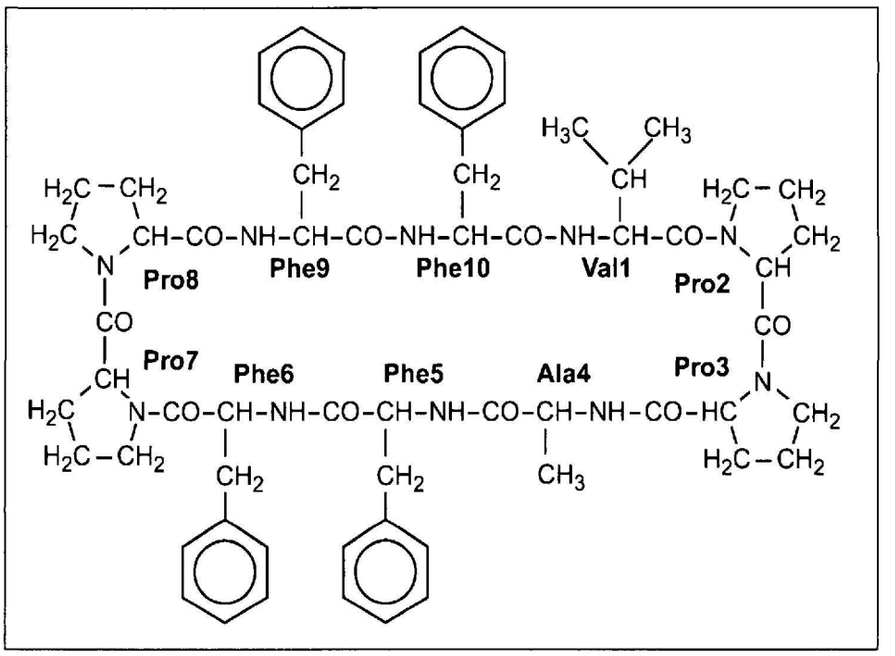

Fig. 2. The antamanide molecule. Antamanide is an exceptionally well-characterized molecule. Here it is used as a test system for evaluating pulse sequences for assignment and structural studies.

35–65 Hz (0.6–1.1 ppm) for the ^{15}N resonances. While this is still about an order of magnitude more than for small proteins in solution, such linewidths allow one to resolve the resonances of peptides much larger than antamanide in multidimensional NMR spectra. Indeed, similar improvements upon recrystallization have been observed in other systems like SH3 (62 residues) [24] and ubiquitin (76 residues) [25], allowing solid-state NMR studies of these systems.

It should be noted that the size and the quality of the resulting microcrystals may be far from sufficient for X-ray diffraction. While X-ray diffraction requires *long-range* order over the entire crystal size of at least several *micro*meters, the only requirement for high-resolution solid-state NMR spectra is *local* order, ensuring that all molecules in the sample sense essentially the same local environment. Solid-state NMR spectra are almost completely insensitive to disorder on a scale beyond a few *nano*meters. There is, thus, a realistic hope that spectra of a similar quality can be obtained from samples for which X-ray quality crystals cannot be grown.

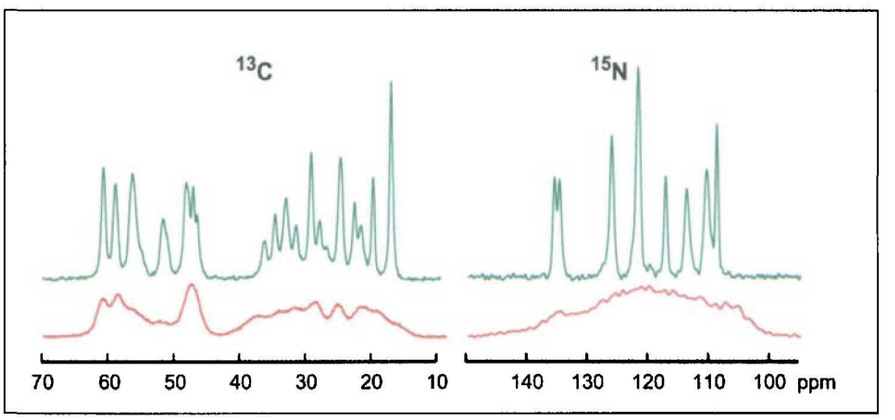

Fig. 3. One-dimensional ^{13}C and ^{15}N MAS spectra of antamanide for two different sample preparation techniques. Red traces: Lyophilized powder. Green traces: Microcrystalline powder obtained by evaporation of the solvent from a solution of antamanide in a methanol/water 7:3 mixture. The microcrystalline powder leads to significantly narrower peaks and a correspondingly higher resolution. The spectra demonstrate the importance of careful sample preparation, resulting in a well-defined, homogeneous local structure. Adapted from [19].

3. Amino-acid Specific Resonance Assignment by Homonuclear Correlation Spectroscopy

The general approach to resonance assignment in high-resolution solid-state NMR is in many respects similar to that used in liquid-state NMR: In a multi-dimensional experiment the resonance frequencies of several spins are correlated by coherence transfer between them. As an example, Fig. 4a shows the general pulse sequence for a two-dimensional (2D) homonuclear correlation experiment under MAS. Initial coherence on the ^{13}C spins is generated by cross polarization. The initial coherence is allowed to evolve for a time period t_1 which is systematically incremented. In the following mixing period, a pulse sequence is applied to the ^{13}C spins to transfer coherence to other spins. The resulting coherences are detected during the time period t_2. Two-dimensional Fourier transformation with respect to the times t_1 and t_2 yields a two-dimensional correlation spectrum [26] (Fig. 4b). If coherence has been transferred from spins with chemical shift δ_A to spins with chemical shift δ_B, a cross peak appears at the position ($\delta_2=\delta_B$, $\delta_1=\delta_A$) in the 2D correlation map (red peaks in Fig. 4b).

In high-resolution solid-state NMR, the spin-spin coupling responsible for polarization transfer can either be the J coupling or the dipolar coupling. The J couplings are only present between spins connected by chemical bonds and are usually strongest between direct neighbors. In liquid-state NMR, methods utilizing the J coupling are used to establish a coupling network between all directly bonded spins within an amino-acid residue. In analogy to the solution-state TOCSY experiment (total correlation spectroscopy [27]), in solid-state NMR such methods are called TOBSY (total through-bond correlation spectroscopy) [28].

In order to achieve TOBSY polarization transfer, only the J coupling must be active during the mixing period, and the chemical shift and the homonuclear and heteronuclear dipolar couplings must be suppressed during this time. These unwanted interactions are often two to three orders of magnitude larger than the J coupling. Efficient suppression can be achieved by irradiating the spins with a suitable pulse sequence in a similar way to the liquid-state TOCSY experiment. However, in solid-state NMR under MAS, care must be exercised in order to avoid the reintroduction of unwanted interactions like CSA or dipolar couplings by interference of the pulse sequence with the MAS rotation. Such recoupling conditions [29–32] lead to stringent design requirements for TOBSY sequences.

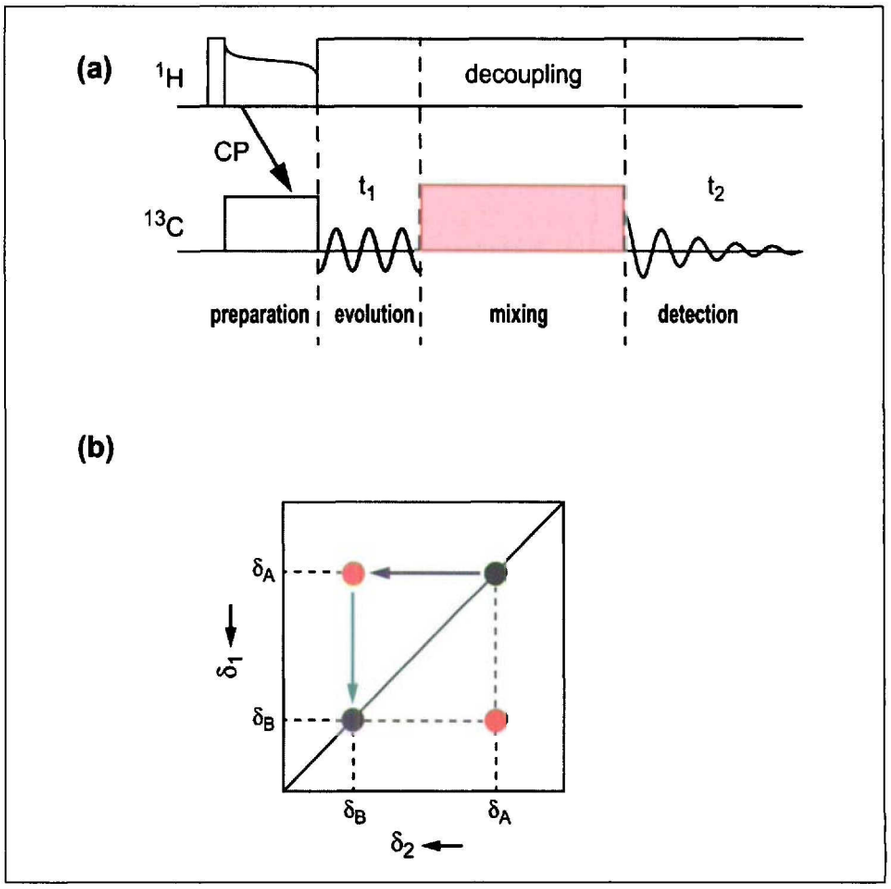

Fig. 4. (a) Pulse scheme for a two-dimensional homonuclear polarization transfer experiment under MAS. Initial coherence on the ^{13}C spins is prepared by cross polarization (CP) from the protons. The coherence is allowed to evolve during a variable time t_1, while the protons are decoupled by a suitable decoupling sequence (here: TPPM). During the mixing time a suitable pulse sequence is applied which induces coherence transfer. After the mixing time, the resulting FID is observed during the detection time t_2, again under proton decoupling. Through the polarization transfer, some coherence which has evolved during t_1 at a chemical shift δ_A (indicated by the blue sinusoid) will be detected at a different chemical shift δ_B (indicated by the green sinusoid). In the 2D spectrum, sketched in part (b), this expresses itself in a cross peak (indicated in red) at the positions ($\delta_2=\delta_B$, $\delta_1=\delta_A$).

We have recently developed a set of TOBSY sequences that are particularly well suited for applications at high MAS frequencies. As an example, a homonuclear 2D chemical-shift correlation spectrum of the cyclic decapeptide antamanide recorded with one of these sequences at an MAS frequency of 30 kHz is shown in Fig. 5. Each cross peak indicates through-bond polarization transfer between two spins; these two spins belong to the same J coupling network within a specific amino acid residue. The spectrum thus allows us to assign all resonances to amino acid types [19]. These assignments are indicated in Fig. 5. Apart from the overall larger linewidths, the spectrum is very similar to a liquid-state ^{13}C TOCSY spectrum of antamanide dissolved in chloroform (data not shown).

Polarization transfer can also proceed through the homonuclear dipolar couplings. Unlike the isotropic J couplings, the anisotropic second-rank dipolar couplings are averaged out by the MAS rotation. However, the dipolar couplings can be recovered by applying specifically designed pulse sequences to the spins, which interfere with the averaging by the MAS rotation ('dipolar recoupling'). The key idea is to recover the dipolar couplings only when they are needed, *i.e.* during the mixing time. During the evolution and detection times, the high resolution offered by the MAS averaging is still obtained.

Over the past 15 years, a large number of dipolar recoupling sequences have been developed [8][33]. However, most

CHIMIA 2001, 55, No. 10

of these sequences cannot be applied at high MAS spinning frequencies due to high rf-field requirements imposed by the sequences. A notable exception is the DREAM (dipolar recoupling enhanced by amplitude modulation) sequence [34][35]. This sequence requires comparatively low rf-field amplitudes, and the performance becomes better at higher MAS frequencies. An important property of the DREAM sequence is that it induces polarization transfer *adiabatically*. Adiabatic sequences for polarization transfer are generally more robust than their non-adiabatic counterparts, and they often lead to significantly higher transfer efficiencies [35–37].

Dipolar couplings are through-space couplings and not through-bond couplings like the J couplings. They can, therefore, connect spins which are close in space but not close in a topological sense and which need not be connected by chemical bonds. However, the strength of the dipolar coupling has a r^{-3} distance dependence which favors nearby spins which are often the directly bonded ones. This is the reason that dipolar recoupling sequences can be used for resonance assignment in much the same way as TOBSY sequences.

The use of a dipolar recoupling sequence for resonance assignment is illustrated in Fig. 6, where a 2 D correlation spectrum of a uniformly ^{13}C and ^{15}N labeled SH3 sample, obtained with the DREAM sequence, is shown. The spectrum was recorded at an MAS frequency of 20.5 kHz. Because of the limited bandwidth of the DREAM sequence at such a relatively low MAS frequency, only a region of the spectrum is recoupled efficiently. By placing the transmitter to 39 ppm, the C^{α} and aliphatic sidechain regions (10–70 ppm) were selected here. At MAS frequencies above 40 kHz, howev-

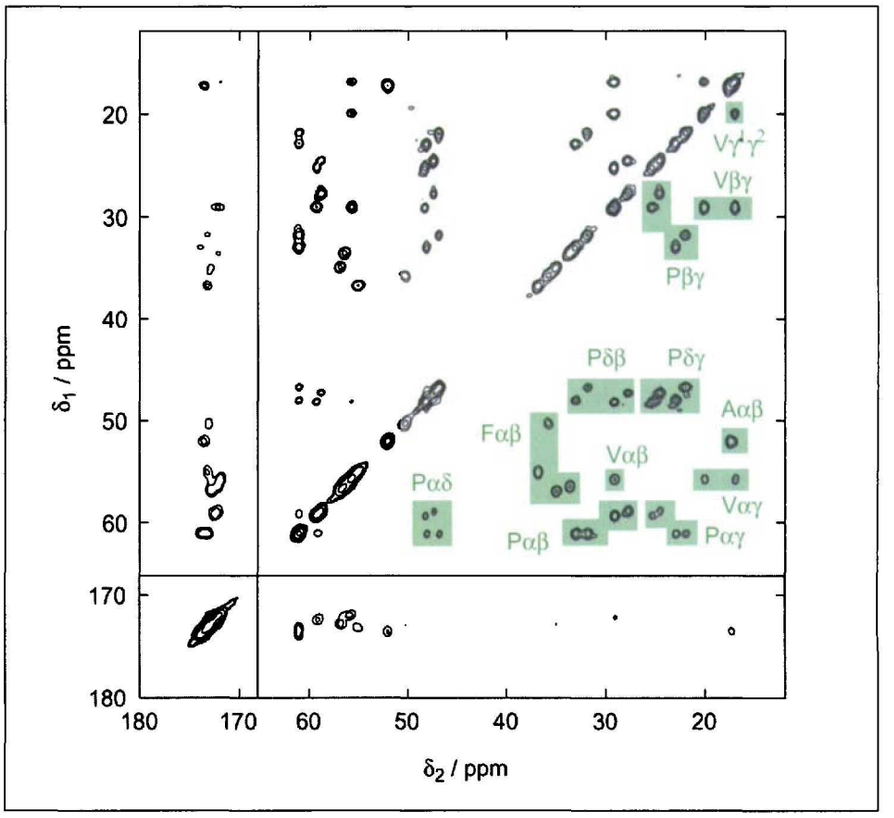

Fig. 5. Homonuclear ^{13}C shift correlation spectrum of antamanide. Polarization transfer was achieved *via* the J couplings by the TOBSY sequence $P9^{1}_{t2}$ at 30 kHz MAS frequency. The spectrum yields cross peaks between the shifts of all ^{13}C spins in the same spin system, which here is identical with an amino acid residue. By this, all resonances can be assigned to their respective amino-acid spin systems. These assignments are indicated in the figure. Adapted from [19].

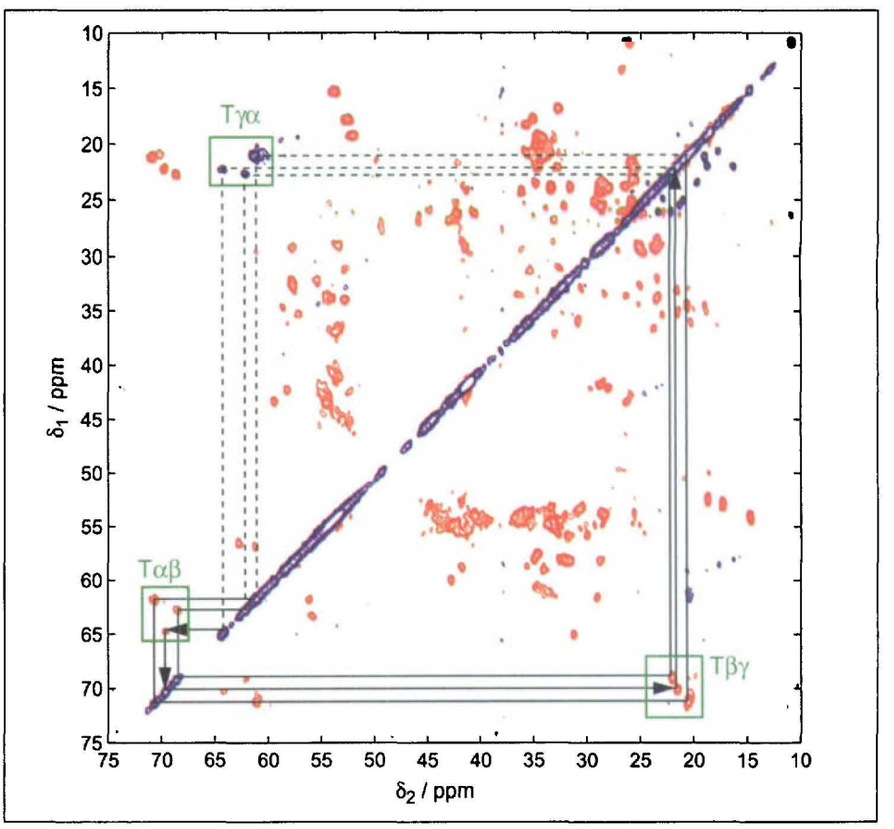

Fig. 6. Homonuclear ^{13}C correlation spectrum of the chicken α-spectrin SH3 domain. Polarization transfer was effected *via* dipolar couplings by the DREAM sequence at 20.5 kHz MAS. The spectrum allows one to perform spin-system assignments in much the same way as in Fig. 5. This is indicated by the solid lines for the three detectable threonine residues. The broken lines indicate correlations between the γ and α carbons, which are separated by the intermediate β carbon. These 'relayed' correlations lead to positive cross peaks, indicated by blue contours, while direct correlations between next neighbors yield negative cross peaks (red contours).

er, the complete spectrum would be recoupled. Due to the larger size of the protein, the spectrum has more resonances and is more complicated in the selected region than the antamanide spectrum of Fig. 5. Nevertheless, the spectrum allows us to assign many of the resonances to their amino-acid spin systems. The resonance assignments for SH3 using solid-state NMR were first reported by Pauli *et al.* [24].

4. Sequence-specific Resonance Assignment by Heteronuclear Correlation Spectroscopy

The homonuclear correlation experiments discussed above identify the resonances that belong to the spin system of one amino acid. This often identifies the type of amino acid (*e.g.* phenylalanine). In order to accomplish a complete sequence-specific resonance assignment (*e.g.* to assign the resonances to phenylalanine 3), the connectivities between the amino-acid residues are required. This information identifies the next as well as the previous amino acid of a certain amino acid in the primary sequence. We therefore need methods that correlate carbon spins across a C'–N–C^{α} peptide bond. This can be achieved by polarization transfer from/to the ^{15}N spin employing heteronuclear ^{15}N-^{13}C polarization transfer techniques.

In the simplest such experiment, initial coherence is created on the amide ^{15}N spins, allowed to evolve, and then transferred to the ^{13}C spins to both sides of the nitrogen. This is illustrated for antamanide in the spectrum shown in Fig. 7a. At the ^{15}N chemical shift of each amide nitrogen along δ_1, the spectrum shows two peaks along δ_2, one at the chemical shift of the $^{13}C'$ directly bonded to the ^{15}N, and one at the chemical shift of the $^{13}C^{\alpha}$ directly bonded to the ^{15}N. Thereby, a correlation between the $^{13}C'$ of one amino-acid residue and the $^{13}C^{\alpha}$ of the next residue is established *via* the linking amide nitrogen.

While a full sequential assignment would in principle be possible by combining the information from the N-C correlation spectrum in Fig. 7a and the TOBSY spectrum in Fig. 5, this goal can be achieved in a more unambiguous way by a method which directly correlates the resonances of the $^{13}C^{\alpha}$ spins in successive residues in a pairwise fashion. For this, we again employ the intermediate amide ^{15}N spin. We already have a correlation of the amide nitrogen to the directly bonded $^{13}C^{\alpha}$ in the *same* residue (Fig. 7a). For establishing a correlation to the $^{13}C^{\alpha}$ of the *preceding* residue, we employ a directed two-step transfer (insert of Fig. 7b). In a first step, polarization is selectively transferred from the ^{15}N to the directly bonded $^{13}C'$. From there, the polarization is transferred – again selectively – to the $^{13}C^{\alpha}$ which is directly bonded to the $^{13}C'$. We call this sequence an N(CO)CA sequence. The resulting spectrum for antamanide is displayed in Fig. 7b, plotted with red contours. For each ^{15}N amide chemical shift, the spectrum shows one cross peak at the chemical shift of the $^{13}C^{\alpha}$ of the preceding amino-acid residue.

By comparing the N(CO)CA spectrum with the 'direct' N-C spectrum of Fig. 7a (indicated by blue areas in Fig. 7b), the $^{13}C^{\alpha}$ resonances of each pair of sequential amino-acid residues can be correlated. These correlations now allow an unambiguous sequential assignment of the $^{13}C^{\alpha}$ resonances by stepping through the cross peaks of the two spectra in the way indicated by the black arrows in Fig. 7b. Once the $^{13}C^{\alpha}$ resonances are assigned in a sequence-specific manner,

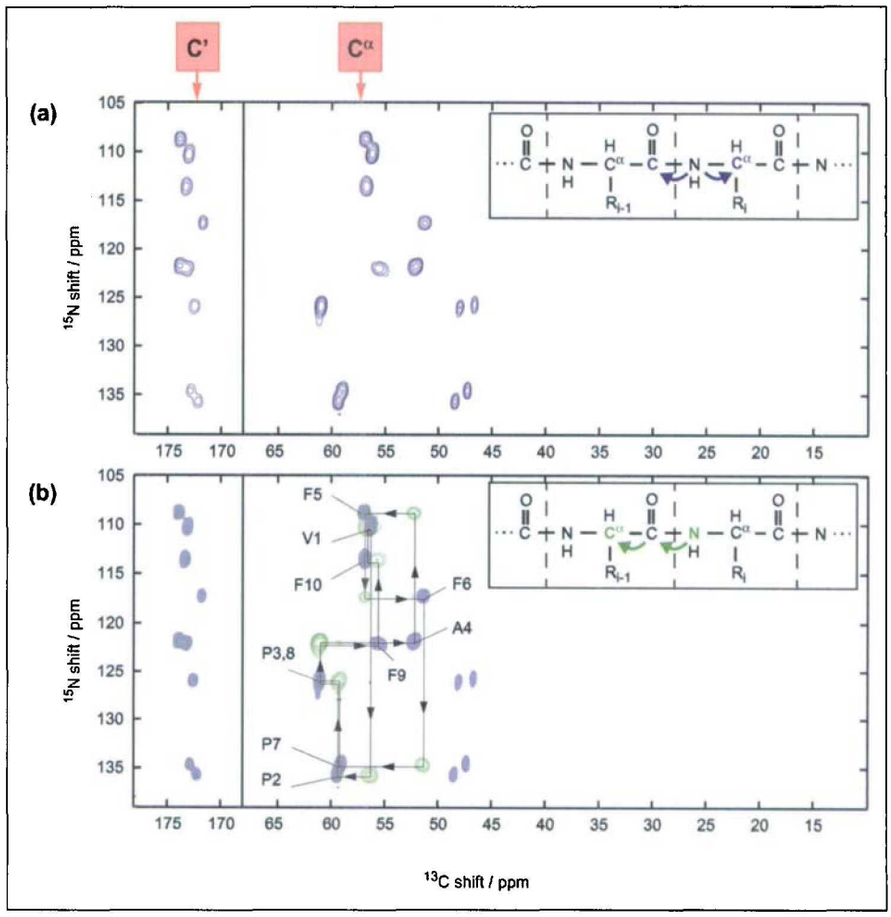

Fig. 7. ^{15}N-^{13}C correlation spectra of antamanide. (a) Direct N-C correlation. Polarization is created on the amide nitrogens and transferred to the directly attached carbons as indicated by the arrows in the insert. (b) N(CO)CA correlation. Polarization is created on the amide nitrogens and then transferred in two successive steps via the $^{13}C'$ to the $^{13}C^{\alpha}$ spins in the previous residue (see insert). The resulting spectrum is shown in red contours. The peak positions of the spectrum of part (a) are indicated by light blue areas. By 'walking' through these two spectra in a stepwise fashion as indicated by the arrows, all ^{15}N and ^{13}C resonances can be assigned in a sequence-specific manner. Adapted from [19].

all other resonances can also be assigned sequentially by the spin-system assignments obtained from the TOBSY spectrum in Fig. 5.

For antamanide, just one homonuclear 2D TOBSY spectrum and two heteronuclear 2D N-C correlation spectra were needed to complete a full resonance assignment. In more complicated cases, *i.e.* larger molecules, the assignment might not be as straightforward. In such cases, the described sequences can easily be modified to include other correlations, *e.g.* by transferring polarization from each amide nitrogen *via* the directly bonded $^{13}C^{\alpha}$ into the sidechains of the polypeptide. Sequences with two-step polarization transfer can easily be extended to include a second evolution period between the transfer steps, leading to the possibility of 3D spectroscopy [19][26][38]. In this way, sequence-specific assignments can be completed for much larger peptides than antamanide. Indeed, two-dimensional experiments similar to the ones discussed here have been reported for the 62-residue SH3 domain by the group of H. Oschkinat and – as already mentioned – have led to a nearly complete assignment of the resonances in that system [23]. This shows that a scaling up of the methods described here is certainly possible and offers prospects for assigning still larger proteins.

5. Perspectives for Future Work

This contribution is focused on experiments directed towards an assignment of the ^{13}C and ^{15}N resonances in polypeptides by high-resolution solid-state NMR. Similar methods have been used so far to partially assign proteins of up to 76 amino acid residues [23][39–41], with work on larger proteins being under way. While all solid-state NMR resonance assignments of uniformly labeled proteins which have so far been reported in the literature were for systems for which also X-ray or liquid-state NMR structures exist, there is reasonable hope that these methods may be applied in a similar fashion also to proteins which are not accessible by these methods. Interesting classes of compounds that may become accessible are membrane-bound proteins and structural proteins (*e.g.* keratin, elastin, silk). The reason for such a hope is that no long-range order is required to obtain well-resolved solid-state NMR spectra. What is needed is a structural homogeneity in the sense that all molecular regions of interest sense the same *local* environment. For the inner regions of a large protein, such a well-defined local environment might already be provided by the rigid secondary and tertiary structure of the molecule itself, without the need for any crystalline order *between* molecules.

While sequence-specific resonance assignments represent a major first step towards structure determination of proteins by high-resolution solid-state NMR, no full structure determination of a protein has yet been published. What are the hurdles to be taken? There is certainly no short answer to this question, but we would like to point out what seems to be the key difficulty towards this goal.

To obtain structural constraints, it is necessary to establish correlations between distant spins, *e.g.* between spins in two different residues which are well separated along the primary sequence, but which are spatially close to each other because of the secondary or tertiary structure. Ideally, one would like to measure the distances between many such spin pairs. This is presently possible with reasonable precision for selectively labeled samples in which only a single distant spin is present. In an uniformly labeled sample, however, there are always spins which are much closer and have, therefore, a much stronger dipolar coupling to at least one of the two spins of a distant spin pair. This stronger coupling often prevents efficient polarization transfer between the two spins of the weakly coupled distant spin pair. Even though some interesting suggestions have recently been made, no general recipe of how to measure long distances in uniformly labeled proteins has yet emerged. We are however optimistic, that this goal can be achieved within the next few months or years.

Solid-state NMR, and especially high-resolution solid-state MAS NMR, is currently in a stage of rapid development, and it appears not unreasonable to expect significant further advances over the course of the next years. There is reasonable hope that entirely new classes of proteins will become accessible to structure determination through solid-state NMR or through its cousin, NMR of proteins in oriented bilayers.

6. Experimental

6.1. *Samples*

Uniformly labeled (U-^{13}C, ^{15}N) antamanide was kindly synthesized by Prof. M. Kainosho (Tokyo) in collaboration with Dr. T. Kawakami and Prof. S. Aimoto. The lyophilized material was recrystallized from a solution of methanol/water 7:3. Approximately 10 mg of the resulting microcrystalline material were packed into a standard 2.5 mm MAS rotor. A 2.5 mm rotor containing approximately 8 mg microcrystalline (U-^{13}C, ^{15}N) protein containing the chicken α-spectrin SH3 domain was kindly provided by Dr. J. Pauli and Prof. H. Oschkinat (Berlin).

6.2. *NMR*

Experiments were performed on a Bruker DMX 600 spectrometer operating at a static magnetic field of 14.1 Tesla. For all experiments, initial ^{13}C or ^{15}N coherence was generated by cross polarization from the protons, employing APHH CP [36][37]. During the evolution and detection periods, high-power proton decoupling with field strengths of 150 kHz (antamanide) and 100 kHz (SH3), respectively, was applied, using the TPPM scheme [42]. Homonuclear 2D correlation experiments on antamanide were performed at 30 kHz MAS frequency employing the $P9^1_{12}$TOBSY sequence for polarization transfer between ^{13}C spins [43]. The mixing time was 10.8 ms; on-resonance proton decoupling at 150 kHz field was applied during the $P9^1_{12}$ sequence. Heteronuclear 2D correlation experiments on antamanide were performed at 20 kHz MAS, employing APHH CP (30 kHz ^{15}N field, 8 ms contact time, Lee-Goldburg decoupling at 150 kHz) for polarization transfer from ^{15}N to ^{13}C [44]. The rotational-resonance tickling (R^2T) sequence (4.5 ms mixing time, 150 kHz on-resonance proton decoupling) was used for further homonuclear transfer [45–47]. More details for the experiments on antamanide are given in [19]. A DREAM experiment was performed on SH3, with parameters as follows: 20.5 kHz MAS frequency, ^1H-^{13}C APHH CP of 1 ms at 50 kHz ^{13}C field. 4.5 ms DREAM mixing with Lee-Goldburg decoupling at 100 kHz. $512t_1$ increments were recorded with a spectral width of 33.3 kHz and 64 transients per increment.

Acknowledgements

We wish to thank Dr. J. Pauli and Prof. H. Oschkinat for a sample of microcrystalline (U-^{13}C, ^{15}N) SH3 protein. We thank Prof. B. Jaun (Organic Chemistry, ETH Zürich) for recording a ^{13}C-TOCSY of the antamanide sample dissolved in $CDCl_3$. Scientific discussions with and contributions from Dr. R. Verel, Dr. E. Hardy, A. Verhoeven, Dr. P. Williamson, Dr. M. Tomaselli, G. Zandomeneghi, L. Beaulieu, J.

van Beek and M. Nijman have been instrumental. Support from the ETH Zurich and the Swiss National Science Foundation are kindly acknowledged

Received: August 15, 2001

[1] R. Huber, *Angew. Chem. Int. Ed. Engl.* **1989,** *28*, 848–869.
[2] K. Wüthrich, 'NMR of Proteins and Nucleic Acids'. Wiley Interscience, New York, **1986**.
[3] J. Cavanagh, W.J. Fairbrother, A.G. Palmer, N.J. Skelton, 'Protein NMR Spectroscopy', Academic Press, San Diego, **1996**.
[4] K. Pervushin, R. Riek, G. Wider, K. Wuthrich, *Proc. Nat. Acad. Sci. U.S.A.* **1997,** *94*, 12366–12371.
[5] K. Pervushin, *Q. Rev. Biophys.* **2000,** *33*, 161–197.
[6] J.D. van Beek, L. Beaulieu, H. Schaefer, M. Demura, T. Asakura, B.H. Meier, *Nature* **2000,** *405*, 1077–1079.
[7] E.R. Andrew, A. Bradbury, R.G. Eades, *Nature* **1958,** *182*, 1659.
[8] R.G. Griffin, *Nature Struct. Biol.* **1998,** *5 supplement*, 508–512.
[9] S.O. Smith, K. Aschheim, and M. Groesbeek, *Q. Rev. Biophys.* **1996**, *29*, 395–449.
[10] B. Reif, M. Hohwy, C.P. Jaroniec, C.M. Rienstra, R.G. Griffin, *J. Magn. Reson.* **2000,** *145*, 132–141.
[11] M. Hong, J.D. Gross, R.G. Griffin, *J. Phys. Chem. B* **1997,** *101*, 5869–5874.
[12] P.R. Costa, J.D. Gross, M. Hong, R.G. Griffin, *Chem. Phys. Lett.* **1997,** *280*, 95–103.
[13] X. Feng, M. Eden, A. Brinkmann, H. Luthman, L. Eriksson, A. Graslund, O.N. Antzutkin, M.H. Levitt, *J. Am. Chem. Soc.* **1997,** *119*, 12006–12007.
[14] T. Wieland, *Angew. Chem. Int. Ed. Engl.* **1968,** *7*, 204–208.
[15] T. Wieland, H. Faulstich, *Crit. Rev. Biochem.* **1978,** *5*, 185–260.
[16] I.L. Karle, T. Wieland, D. Schermer, H.C.J. Ottenheym, *Proc. Nat. Acad. Sci. U.S.A.* **1979,** *76*, 1532–1536.
[17] H. Kessler, J.W. Bats, J. Lautz, A. Muller, *Justus Liebigs Ann. Chem.* **1989**, 913–928.
[18] H. Kessler, A. Muller, K.H. Pook, *Justus Liebigs Ann. Chem.* **1989**, 903–912.
[19] A. Detken, E.H. Hardy, M. Ernst, M. Kainosho, T. Kawakami, S. Aimoto, B.H. Meier, *J. Biomol. NMR* **2001**, *20*, 203–221.
[20] C.A. Koch, D. Anderson, M.F. Moran, C. Ellis, T. Pawson, *Science* **1991,** *252*, 668–674.
[21] A. Musacchio, M. Noble, R. Pauptit, R. Wierenga, M. Saraste, *Nature* **1992,** *359*, 851–855.
[22] F.J. Blanco, A.R. Ortiz, L. Serrano, *J. Biomol. NMR* **1997,** *9*, 347–357.
[23] J. Pauli, M. Baldus, B. van Rossum, H. de Groot, H. Oschkinat, *Chem. Bio. Chem.* **2001,** *2*, 272–281.
[24] J. Pauli, B. van Rossum, H. Forster, M. de Groot, H.J, H. Oschkinat, *J. Magn. Reson.* **2000,** *143*, 411–416.
[25] T.I. Igumenova, R. Martin, C. Rienstra, E. Paulson, A.J. Wand, K.W. Zilm, A.E. McDermott. Poster at the 42nd Experimental Nuclear Magnetic Resonance Conference, Orlando, Florida, March 11–16, **2001**.
[26] R.R. Ernst, G. Bodenhausen, A. Wokaun, 'Principles of Nuclear Magnetic Resonance in One and Two Dimensions', Clarendon Press, Oxford, **1987**.
[27] L. Braunschweiler, R.R. Ernst, *J. Magn. Reson.* **1983,** *53*, 512.
[28] M. Baldus, B.H. Meier, *J. Magn. Reson. Series A* **1996,** *121*, 65–69.
[29] T.G. Oas, R.G. Griffin, M.H. Levitt, *J. Chem. Phys.* **1988,** *89*, 692.
[30] M.H. Levitt, T.G. Oas, R.G. Griffin, *Isr. J. Chem.* **1988,** *28*, 271–282.
[31] M.G. Colombo, B.H. Meier, R.R. Ernst, *Chem. Phys. Lett.* **1988,** *146*, 189.
[32] N.C. Nielsen, H. Bildsoe, H.J. Jakobsen, M.H. Levitt, *J. Chem. Phys.* **1994**, *101*, 1805.
[33] M. Baldus, D.G. Geurts, B.H. Meier, *Solid State NMR* **1998,** *11*, 157–168.
[34] R. Verel, M. Baldus, M. Ernst, B.H. Meier, *Chem. Phys. Lett.* **1998,** *287*, 421–428.
[35] R. Verel, M. Ernst, B.H. Meier, *J. Magn. Reson.* **2001,** *150*, 81–99.
[36] S. Hediger, B.H. Meier, N.D. Kurur, G. Bodenhausen, R.R. Ernst, *Chem. Phys. Lett.* **1994,** *223*, 283–288.
[37] S. Hediger, B.H. Meier, R.R. Ernst, *Chem. Phys. Lett.* **1995,** *240*, 449.
[38] B.Q. Sun, C.M. Rienstra, P.R. Costa, J.R. Williamson, R.G. Griffin, *J. Am. Chem. Soc.* **1997**, *119*, 8540–8546.
[39] S.K. Straus, T. Bremi, R.R. Ernst, *J. Biomol. NMR* **1998,** *12*, 39–50.
[40] M. Hong. *J. Biomol. NMR* **1999,** *15*, 1–14.
[41] A. McDermott, T. Polenova, A. Bockmann, K.W. Zilm, E.K. Paulsen, R.W. Martin, G.T. Montelione, *J. Biomol. NMR*, **2000,** *16*, 209–219.
[42] A.E. Bennett, C.M. Rienstra, M. Auger, K.V. Lakshmi, R.G. Griffin, *J. Chem. Phys.* **1995**, *103*, 6951–6958.
[43] E.H. Hardy, R. Verel, B.H. Meier, *J. Magn. Reson.* **2001**, *148*, 459–464.
[44] M. Baldus, D.G. Geurts, S. Hediger, B.H. Meier, *J. Magn. Reson. Series A* **1996,** *118*, 140–144.
[45] K. Takegoshi, K. Nomura, T. Terao, *Chem. Phys. Lett.* **1995,** *232*, 424–428.
[46] K. Takegoshi, K. Nomura, T. Terao, *J. Magn. Reson.* **1997**, *127*, 206–216.
[47] P.R. Costa, B.Q. Sun, R.G. Griffin, *J. Am. Chem. Soc.* **1997**, *119*, 10821–10830.